UNSUPERVISED LEARNING APPLIED TO MINERAL OIL SPILL AND BIOGENIC OIL DISCRIMINATION IN RADARSAT-2 IMAGE

Priscila Martins Oliveira da Costa[1], *Guillaume Lassalle*[2], *Laura Elena Cué La Rosa*[3], *Rebecca Del Papa Moreira Scafutto*[4] *Matheus Pinheiro Ferreira*[5], *and Carlos Roberto de Souza Filho*[6]

[1]Geosciences Institute, University of Campinas, Campinas, SP, Brazil, oliveira.priscilamartins@gmail.com; [2]Geosciences Institute, University of Campinas, Campinas, SP, Brazil, lassalle@unicamp.br; [3]Department of Electrical Engineering, Pontifical Catholic University of Rio de Janeiro (PUC), Rio de Janeiro, RJ, Brazil, lauracue@aluno.puc-rio.br; [5]Geosciences Institute, University of Campinas, Campinas, SP, Brazil, rebecca.scafutto@gmail.com; [6]Cartographic Engineering Department, Military Institute of Engineering (IME), Rio de Janeiro, RJ, Brazil, matheus@ime.eb.br; [7]Geosciences Institute, University of Campinas, Campinas, SP, Brazil, beto@unicamp.br

ABSTRACT

Accurate detection and characterization of offshore oil slicks are essential for decision making in prospection and environmental contexts. The similarity of oil spills from different sources makes their classification in SAR images challenging. In this work, we presented an oil spill clustering model based on RADARSAT-2 image. We developed a model able to distinguish between mineral and biogenic oil based on a state-of-art self-supervised deep clustering algorithm. The Silhouette score and Calinski-Harabasz index were used to define the optimal number of clusters.

Key words *– Oil spill, Synthetic Aperture Radar, Unsupervised Learning, Clustering.*

1. INTRODUCTION

Offshore oil spills are a major threat to the sea ecosystems, endangering marine and coastal life. The oil can occur naturally through natural phenomenon (seepages) or be caused by accidents or failures in the production and transport chain of oil. The development of techniques to assist in the monitoring, identification and characterization of oil is of interest to the scientific, business, and civil communities. Remote Sensing (RS) has demonstrated great applicability for oil slick monitoring, since it allows collecting data and generating information in large spatial extents. Among RS sensors, Synthetic Aperture Radar (SAR) stands out for oil slick detection, due to its operability independent of sunlight and cloud cover and contrasting difference between oil and seawater backscattering [1]. Capillary waves on the ocean reflect radar energy, producing a 'bright' image. In conventional situation, the oil floating on the sea damps the sea surface roughness, reducing the radar signal that returns to the sensor. Thus, the oil appears as black patches in SAR image [2].

However, oil slicks are not the only phenomena that reduces backscattering in SAR images. A series of false targets can present the same pattern in SAR data, such as algae blooms, biogenic oil, and wind speed variations [3]. Due to the difficulty of access and logistics in distant oceanic areas, oil slicks and 'lookalikes' detected in the SAR images are not usually validated in the field. The absence of labelled databases makes the classification of oil spills even more challenging.

The potential of deep learning models to oil spill classification has been greatly demonstrated in the literature [4, 5]. Self-supervised learning strategies emerge as an alternative for supervised feature learning where no label information is available, common in research of this nature. In this context, the objective of this work is to distinguish between mineral oil and biogenic oil in a SAR image, through unsupervised learning strategy. Here, we exploit the potential of a recently proposed self-supervised deep learning algorithm that employs contrastive learning to perform unsupervised feature learning and clustering [6].

2. MATERIAL E METHODS

2.1. Dataset

Between June 6-9, 2011, an experiment with controlled discharges of oil at the North Sea (59°59'N, 2°27'E) was conducted by the Norwegian Clean Seas Association for Operating Companies (NOFO). Three different targets were released on the ocean: oil emulsion, crude oil and plant oil (Table 1). Satellite images were acquired during the experiment, including imagery from RADARSAT-2 satellite. An image acquired on June 8th, 2011, from RADARSAT-2 was used in this work. The detailed description of the experiment can be consulted at [7, 10].

2.2. Methodology

The proposed method is based on the Swapping Assignments between multiple Views (SwAV) method [6], which jointly performs self-supervised feature learning and clustering via combining contrastive learning and an optimal transport theory. The SwAV method assigns the input samples into a set of clusters by forcing an equipartition constraint that ensure that all samples are equally distributed among the clusters. The optimal transport solve preforms the cluster assignment, while contrastive learning ensures that samples that are close in the feature space are assigned to the same cluster. These samples are obtained by applying different transformations to the same input sample. In addition, we implemented a custom data loader that allows working with large-scale radar imagery in an online fashion using only the raw data as input. For more details about the SwAV model we refer the reader to [6].

	Type	Date	Volume
Plant Oil	Radiagreen EBO: a monoalkyl ester of an oleic acid produced from vegetable oils	8 June 2011	0.4 m^3
Emulsion	Oseberg blend crude oil mixed with 5% IFO3801 with a water content of 69% and viscosity of 4860 mPa ·s	7 June 2011	20 m^3
Crude oil	Balder crude oil: density of 0.914 g/mL and dynamic viscosity of 219 mPa ·s	8 June 2011	30 m^3

Table 1. Properties of substances released on sea. According to [7].

2.2.1. Experimental design

The image was pre-processed following the flowchart well established in literature: 1) Calibration to Sigma zero; 2) Multilooking; 3) Speckle Filter; 4) Terrain Correction and 5) Conversion to decibel scale (dB). H/Alpha decomposition [11] was applied to pre-processed image in order to differentiate the backscatter of the three targets. In summary, this technique decomposes the three basics scattering mechanisms by calculating the eigenvalues and eigenvectors of the coherence matrix. As consequence, three parameters are defined: entropy, alpha angle and anisotropy. The entropy measures the degree of randomness or statistical disorder of the scattering process. The alpha angle provides information about scattering mechanism. Finally, anisotropy is a complementary parameter of entropy, and can also be regarded as an indication of small-scale surface roughness [12].

Table 2 summarizes the expected behaviour of sigma zero VV, entropy and alpha angle in mineral oil, plant oil and sea-water. The sigma zero of VV polarization, entropy, anisotropy, alpha angle, amplitude and phase of data were the input to the SwAV model. As the objective of the work is developing a model capable of discriminating between mineral and biogenic oil, a mask was applied to seawater. The mask was built in ENVI 5.2 software [13, 14], extracting the slicks from the image by applying a segmentation algorithm based on a threshold value.

The resultant image with the seawater masked was the input to the model. Our implementation of the SwAV model employs a backbone convolutional neural network based on ResNet18 [15], followed by a fully connected layer that maps the features to a set of predefined prototypes (or clusters centroids). Next, the optimal transport algorithm is employed to perform the cluster assignment following the equipartition condition. We employed random resize crop, flips and rotations as image transformation to augment the training data. To determinate the optimal number of clusters for our task, we trained different models varying the number of clusters from 3 to 50 and selected the optimal one based on the average Silhouette score [16] and Calinski-Harabasz Index [17]. The Silhouette score measures the quality of clustering using the mean intra-cluster distance and the mean nearest cluster distance for each sample. The Silhouette coefficient is defined according to Equation 1:

$$Silhouette\ score = \frac{(b-a)}{max(a,b)} \tag{1}$$

where b is the mean distance between a sample and all other points in the next nearest cluster, and a is the mean distance between a sample and all other points in the same class. The Silhouette score varies from -1 to 1. Score equals to 1 indicates that clusters are dense and well separated. Score equals to -1 means incorrect clustering, and score around zero indicates overlapping clusters. The calculation of Silhouette score is of high computational complexity (n^2 calculations, being n the number of samples). Due to computational limitations, we selected 10% of samples of original data to calculate the average Silhouette score. The average Silhouette score as a function of the number of clusters is shown in Figure 1. The cluster number 5 (i.e., 5 clusters) is the first ascending point, reaching average Silhouette score equal to 0.899. The clusters 11 and 45 got the same value of Silhouette, equals to 0.904.

The Calinski-Harabasz index, also known as the Variance Ratio Criterion, is the ratio of the sum of between-clusters dispersion and of inter-cluster dispersion for all clusters. The higher score means better performance. Figure 1 shows the Calinski-Harabasz index as a function of the number of clusters. Since the index is fast to compute all the samples were used to compute it. Five clusters achieved the higher value, which means that clusters are dense and well separated.

Cluster 5 was chosen as optimal cluster. In Calinski-Harabasz index it was the higher value. The difference between average Silhouette score of clusters 11 and 5 was very low, around 0.005.

3. RESULTS AND DISCUSSION

Figure 2 presents the sigma zero of VV polarization from original RADARSAT-2 image (top) and respective predicted map regarding to 5 clusters (bottom) relative to plant oil, emulsion and crude oil. It is observed that the model revealed differences between biogenic oil (plant) and mineral oil (emulsion and crude oil). The plant oil is well discriminate from other targets. The majority of pixels are from cluster 3. In crude oil and emulsion, it is observed a similar distribution

Feature	Mineral Oil	Plant Oil	Clean seawater
Sigma zero (VV)	Lower than background	Low	High
Entropy (H)	High	Low	Lower than background
Alpha angle	High	Low	Lower than background

Table 2. Expected behavior of sigma zero, entropy and alpha angle at mineral oil, plant oil and clean seawater [3, 8, 9].

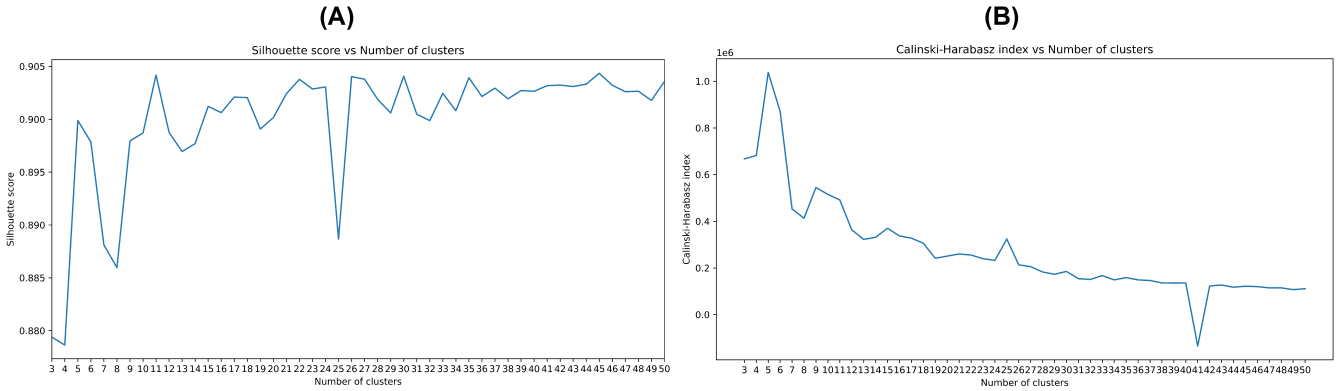


Figure 1. (A) Average Silhouette score in function of number of clusters, (B) Calinski-Harabasz index in function of number of clusters.

of classes, but clusters 0 and 2 predominates over crude oil and class 4 predominates over emulsion.

4. CONCLUSIONS

The potential of unsupervised deep learning model to oil spill discrimination was demonstrated. Despite the presence of similar classes among the targets, the model was able to distinguish between biogenic and mineral oil automatically. For further works, the results will be improved applying a major-voting rule to pixels encompassed by targets. The proposed methodology can be easily replicated for other unlabeled oil spill images.

5. REFERENCES

[1] Werner Alpers, Benjamin Holt, and Kan Zeng. Oil spill detection by imaging radars: Challenges and pitfalls. *Remote Sensing of Environment*, 201:133–147, 2017.

[2] Merv Fingas and Carl Brown. Review of oil spill remote sensing. *Marine Pollution Bulletin*, 83(1):9–23, 2014.

[3] M. Migliaccio, F. Nunziata, and A. Buono. Sar polarimetry for sea oil slick observation. *International Journal of Remote Sensing*, 36(12):3243–3273, 2015.

[4] Kan Zeng and Yixiao Wang. A deep convolutional neural network for oil spill detection from spaceborne sar images. *Remote Sensing*, 12(6), 2020.

[5] Ran Pelta, Nimrod Carmon, and Eyal Ben-Dor. A machine learning approach to detect crude oil contamination in a real scenario using hyperspectral remote sensing. *International Journal of Applied Earth Observation and Geoinformation*, 82:101901, 2019.

[6] Mathilde Caron, Ishan Misra, Julien Mairal, Priya Goyal, Piotr Bojanowski, and Armand Joulin. Unsupervised learning of visual features by contrasting cluster assignments. *Advances in Neural Information Processing Systems*, 2020.

[7] Stine Skrunes, Camilla Brekke, and Torbjørn Eltoft. Characterization of marine surface slicks by radarsat-2 multipolarization features. *IEEE Transactions on Geoscience and Remote Sensing*, 52(9):5302–5319, 2014.

[8] Guandong Chen, Yu Li, Guangmin Sun, and Yuanzhi Zhang. Application of deep networks to oil spill detection using polarimetric synthetic aperture radar images. *Applied Sciences*, 7(10), 2017.

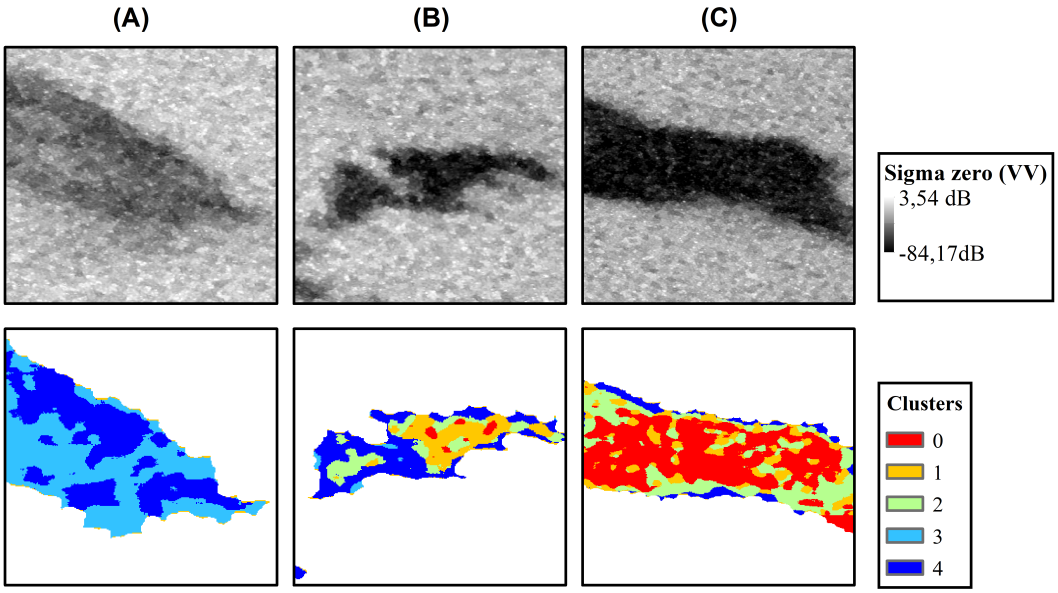


Figure 2. Sigma zero of VV polarization from original RADARSAT-2 image (top) and predicted map regarding to 5 clusters (bottom) from (A) Plant oil, (B) Emulsion and (C) Crude oil.

[9] Yuanzhi Zhang, Yu Li, X. San Liang, and Jinyeu Tsou. Comparison of oil spill classifications using fully and compact polarimetric sar images. *Applied Sciences*, 7(2), 2017.

[10] Dmitry Ivonin, Camilla Brekke, Stine Skrunes, Andrei Ivanov, and Nataliya Kozhelupova. Mineral oil slicks identification using dual co-polarized radarsat-2 and terrasar-x sar imagery. *Remote Sensing*, 12(7), 2020.

[11] S.R. Cloude and E. Pottier. An entropy based classification scheme for land applications of polarimetric sar. *IEEE Transactions on Geoscience and Remote Sensing*, 35(1):68–78, 1997.

[12] Alberto Moreira, Pau Prats-Iraola, Marwan Younis, Gerhard Krieger, Irena Hajnsek, and Konstantinos P. Papathanassiou. A tutorial on synthetic aperture radar. *IEEE Geoscience and Remote Sensing Magazine*, 1(1):6–43, 2013.

[13] Jos B.T.M. Roerdink and Arnold Meijster. The watershed transform: Definitions, algorithms and parallelization strategies. *Fundamenta Informaticae*, 41:187–228, 2000. Relation: http://www.rug.nl/informatica/organisatie/overorganisatie/iwi Rights: University of Groningen. Research Institute for Mathematics and Computing Science (IWI).

[14] Jin Xiaoying. Segmentation-based image processing system, U.S. Patent 8,260,048, filed Nov. 14, 2007, and issued Sept. 4, 2012.

[15] Kaiming He, Xiangyu Zhang, Shaoqing Ren, and Jian Sun. Deep residual learning for image recognition. In *2016 IEEE Conference on Computer Vision and Pattern Recognition (CVPR)*, pages 770–778, 2016.

[16] Peter J. Rousseeuw. Silhouettes: A graphical aid to the interpretation and validation of cluster analysis. *Journal of Computational and Applied Mathematics*, 20:53–65, 1987.

[17] T. Caliński and J Harabasz. A dendrite method for cluster analysis. *Communications in Statistics*, 3(1):1–27, 1974.